On the Thermodynamic Efficiency of Ca^{2+}-ATPase Molecular Machines

Anders Lervik,[†*] Fernando Bresme,[‡†] Signe Kjelstrup,[†§] and J. Miguel Rubí[¶]
[†]Department of Chemistry, Norwegian University of Science and Technology, Trondheim, Norway; [‡]Department of Chemistry, Imperial College, London, United Kingdom; [§]Process and Energy Laboratory, Delft University of Technology, Delft, The Netherlands; and [¶]Departamento de Física Fonamental, Facultat de Física, Universitat de Barcelona, Barcelona, Spain

ABSTRACT Experimental studies have shown that the activity of the reconstituted molecular pump Ca^{2+}-ATPase strongly depends on the thickness of the supporting bilayer. It is thus expected that the bilayer structure will have an impact on the thermodynamic efficiency of this nanomachine. Here, we introduce a nonequilibrium-thermodynamics theoretical approach to estimate the thermodynamic efficiency of the Ca^{2+}-ATPase from analysis of available experimental data about ATP hydrolysis and Ca^{2+} transport. We find that the entropy production, i.e., the heat released to the surroundings under working conditions, is approximately constant for bilayers containing phospholipids with hydrocarbon chains of 18–22 carbon atoms. Our estimates for the heat released during the pump operation agree with results obtained from separate calorimetric experiments on the Ca^{2+}-ATPase derived from sarcoplasmic reticulum. We show that the thermodynamic efficiency of the reconstituted Ca^{2+}-ATPase reaches a maximum for bilayer thicknesses corresponding to maximum activity. Surprisingly, the estimated thermodynamic efficiency is very low, ~12%. We discuss the significance of this result as representative of the efficiency of other nanomachines, and we address the influence of the experimental set-up on such a low efficiency. Overall, our approach provides a general route to estimate thermodynamic efficiencies and heat dissipation in experimental studies of nanomachines.

INTRODUCTION

The calcium pump (Ca^{2+}-ATPase) of the sarcoplasmic reticulum (SR) is a P-type ATPase that actively transports Ca^{2+} from the cytosol to the lumen of the SR using ATP as fuel. During muscle contraction, Ca^{2+} is released from the lumen of the SR to the cytosol, and this induces a conformational change of tropomyosin that allows actin and myosin to form cross-bridges. By pumping Ca^{2+} from the cytosol and back into the lumen of the SR, the Ca^{2+}-ATPase enables the muscles to relax: a conformational change enables tropomyosin to bind to actin, and cross-bridges between actin and myosin can no longer form (1).

The Ca^{2+}-ATPase can be extracted from, for instance, the skeletal muscle of mammals, and reconstituted into a bilayer in which the phospholipid composition can be varied (2). In early experiments, it was noticed that the protein binds with approximately the same affinity to a large variety of phospholipid bilayers, making possible a systematic investigation of protein activity with varying phospholipid chain length, where the activity is estimated in terms of the amount of the Ca^{2+} transported and the amount of ATP hydrolyzed. It was found that the activity reaches a maximum when the protein is inserted into bilayers with a narrow range of lengths for the phospholipid acyl chain hydrocarbon length, typically between 16 and 20 carbon atoms (2–4).

A strong dependence of the transport activity with the phospholipid acyl chain length has been observed in other proteins, e.g., in proton and cation transporters in bacteria (see, e.g., Andersen et al. (4)). The fact that this behavior is observed in structurally different proteins has motivated further study, and several explanations relating the protein activity to the protein-bilayer interactions have been suggested (5). How these interactions modify the structure of the bilayers around the protein and the structure of the protein transmembrane domains remains an open question. Recent computer simulation studies have addressed this question by investigating Ca^{2+}-ATPase embedded in phospholipid liquid crystal phases and targeting bilayer compositions for which maximum activity is observed in the experiments (6,7). These works show that the bilayer membrane deforms around the protein, and that both the protein and the membrane mutually adapt their structures. The simulations indicate that the deformation of the phospholipid membrane may be compatible with optimum pump activity. Although the specific details of the level of deformation of the membrane and structural modifications of the protein are not fully established, it is known that membrane proteins stop functioning when the protein is reconstituted in the phospholipid membrane gel phase (5). Further investigations have also indicated that experimental conditions, in particular pH, play a significant role in determining protein activity, with the activity reaching a maximum in the Ca^{2+} pump at pH 7.5 (8). This behavior could be connected to the sensitivity of the protonation states of the amino acids to pH conditions. In fact, a recent work on Ca^{2+}-ATPase has highlighted the sensitivity of Ca^{2+} binding to pH conditions (9).

In addition to the studies referred to above, experiments by de Meis's group (10–17) have shown that while the Ca^{2+}-ATPase is embedded in vesicles derived from SR, it

Submitted May 15, 2012, and accepted for publication July 16, 2012.

*Correspondence: anders.lervik@chem.ntnu.no

Editor: Robert Nakamoto.

0006-3495/12/09/1218/9 $2.00

http://dx.doi.org/10.1016/j.bpj.2012.07.057

dissipates heat, and that hence, at least under the experimental conditions, it is an imperfect pump. Calorimetric measurements have shown that under working conditions the protein might transport heat reversibly in addition to dissipating energy (11). This notion seems to be compatible with recent experiments on ATPase reconstituted into vesicles, from which one can infer the creation of temperature gradients of the order of 10^4–10^5 K/m when the pump is under working conditions (18). These large gradients that involve modest temperature differences, ~1 K over micrometer length scales, could in principle lead to interesting nonequilibrium effects in solution (19,20).

The experimental studies reported above have motivated a number of theoretical works aimed at explaining the Ca^{2+} transport process using nonequilibrium thermodynamics (NET) theory (21,22). One advantage of NET theory is that it provides a theoretical framework to rationalize the transport process in terms of phenomenological coefficients, which can be measured using suitable experiments. Kjelstrup et al. (23) performed such analyses. By interpreting experimental data by de Meis and co-workers (10–17), they showed that the magnitude of the phenomenological coefficients depends on the protein isomorph, so that proteins present in white skeletal muscle and brown adipose tissue are more efficient at releasing heat in their surroundings. Overall, experiments indicate that the hydrolysis of ATP provides energy to transport ions, but there is evidence that ATPases are more effective transporters when they are immersed in the right membrane and for certain initial conditions. The energy that is not being utilized for the transport process is dissipated. Indeed, as noted above, there is experimental evidence that this transport and dissipation can lead to temperature gradients. To understand the working conditions of these nanomachines and what makes them more or less efficient, it is important to quantify this efficiency on thermodynamic grounds. We tackle this problem here with the help of NET theory, which has been successfully employed recently to interpret experimental data (23).

This article is structured as follows. We first describe the ATPase system, and the necessary NET equations. We then use NET theory to analyze the experimental results of Caffrey and Feigenson (2) for the reconstituted pump activity and quantify the thermodynamic efficiency of the pump as a function of the bilayer thickness. We close with a section containing the main conclusions and final remarks.

THE CA^{2+}-ATPase

Let us consider the Ca^{2+}-ATPase protein embedded in the biological membrane of a vesicle, as depicted in Fig. 1. The system consists of three parts (22): the external phase (out), the membrane phase, and the internal phase (in). The external and internal phases form the boundary conditions. The membrane phase consists of a semipermeable lipid bilayer

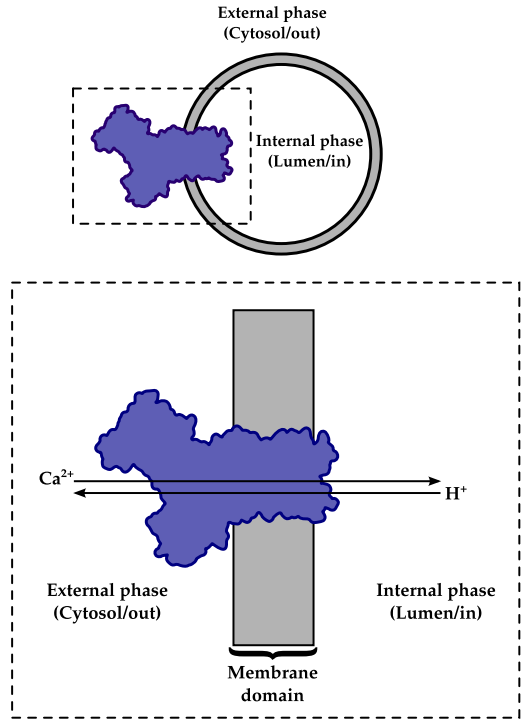

FIGURE 1 Sketch of the Ca^{2+}-ATPase protein embedded in a vesicle/phospholipid membrane. The Ca^{2+}-ATPase is drawn in blue and the bilayer in gray. (*Upper*) The vesicle shown with only one protein in exaggerated size for clarity. (*Lower*) Enlargement of dashed-box area in upper image, where the arrows illustrate the direction in which the ions are transported under the normal operation of the pump. The positive direction for transport is from the external phase (*cytosol/out*) to the internal phase (*lumen/in*).

with the embedded Ca^{2+}-ATPase and the adsorbed species: water, ions, and the reactants and products of the ATP hydrolysis. The hydrolysis of ATP is represented by (24,25)

$$\mathrm{ATP} + \mathrm{H_2O} \rightleftharpoons \mathrm{ADP} + \mathrm{P_i}, \tag{1}$$

where ATP, ADP, and P_i are adenosine triphosphate, adenosine diphosphate, and inorganic phosphate, respectively. The energy from ATP hydrolysis can be used to exchange ions. The Ca^{2+}-ATPase is electrogenic and countertransports two to three H^+/two Ca^{2+} (26,27). However, the exchange of ions may still be electroneutral. The SR membrane is highly permeable to K^+ and this is the likely cause of a membrane potential maintained near zero (28,29). The membrane is also permeable to other ions, e.g., H^+ (29,30). Tran et al. (31) have argued that the formation of a steady-state H^+-gradient under biological conditions is unlikely, since the SR vesicle membrane is highly permeable to protons (32). Based on this, we neglect the membrane potential in our description and assume that there exist pathways (besides active pumping) for transport of other ions, making the operation of the pump electroneutral. For the pump derived from SR, this is a good assumption, whereas it is more questionable for the reconstituted pump. However, in this case, there is also some

back-transport of H^+ via the pump itself. We therefore assume that the electroneutrality is fulfilled by H^+ and we do not consider transport of other ions. Hence, we represent the exchange of ions by

$$Ca^{2+}(\text{out}) + 2H^+(\text{in}) \rightleftharpoons Ca^{2+}(\text{in}) + 2H^+(\text{out}), \quad (2)$$

where out refers to the external phase (the cytosol) and in refers to the internal phase (the lumen). A typical concentration difference corresponds to a ratio of the calcium concentration in the lumen to that in the cytosol of 10^4 (1). The exchange of two Ca^{2+} ions corresponds, then, to a Gibbs energy of $\sim 2 \times RT \ln 10^4 \approx 47$ kJ/mol at 37°C if we assume that the pH is the same on both sides.

Considering this and the Gibbs energy of the ATP hydrolysis, which is ~−50 kJ mol^{-1} for physiological conditions (1), the net change in Gibbs energy is negative, and the pump should transport calcium ions from the cytosol to the lumen at the expense of the ATP hydrolysis. If only one Ca^{2+} is transported, half the energy is dissipated. With a positive net change in Gibbs energy, the pump will operate in the reverse direction and synthesize ATP molecules, using the energy stored in the Ca^{2+} concentration gradient.

NONEQUILIBRIUM THERMODYNAMIC DESCRIPTION OF THE SYSTEM

Nonequilibrium thermodynamics describes the pump through the entropy production and a set of equations relating the fluxes and driving forces. The steady-state operation of the ion pump is described by the flux-force relations (22),

$$\begin{aligned}
J_{Ca^{2+}} &= -D_{dr}\left[1 - \exp\left(-\frac{\Delta_r G}{RT^{out}}\right)\right] + D_{dd}\left[1 - \exp\left(\frac{\Delta\mu_{Ca^{2+}/2H^+}}{RT^{out}}\right)\right] - \frac{D'_{dq}}{RT^{out}}\left(1 - \frac{T^{out}}{T^{in}}\right),\\
r &= -D_{rr}\left[1 - \exp\left(-\frac{\Delta_r G}{RT^{out}}\right)\right] + D_{rd}\left[1 - \exp\left(\frac{\Delta\mu_{Ca^{2+}/2H^+}}{RT^{out}}\right)\right] - \frac{D'_{rq}}{RT^{out}}\left(1 - \frac{T^{out}}{T^{in}}\right),\\
J'^{out}_q &= -D'_{qr}\left[1 - \exp\left(-\frac{\Delta_r G}{RT^{out}}\right)\right] + D'_{qd}\left[1 - \exp\left(\frac{\Delta\mu_{Ca^{2+}/2H^+}}{RT^{out}}\right)\right] - \frac{D'_{qq}}{RT^{out}}\left(1 - \frac{T^{out}}{T^{in}}\right),
\end{aligned} \quad (3)$$

where $J_{Ca^{2+}}$ is the flux of calcium ions, r is the rate of ATP hydrolysis, and J'^{out}_q is the heat flux associated with a temperature gradient across the bilayer. Here, the fluxes are given as exponential functions of the driving forces, as is typical for activated processes (33). The driving forces for the reaction $(-\Delta_r G/T^{in})$ and the exchange of ions $(-\Delta\mu_{Ca^{2+}/2H^+}/T^{in})$ are given by the Gibbs energy of the ATP reaction (see Eq. 1),

$$\Delta_r G = \mu_{ADP} + \mu_{Pi} - \mu_{ATP} - \mu_{H_2O}, \quad (4)$$

and the change in chemical potential on moving ions between the cytosol and the lumen of the vesicle (see Eq. 2),

$$\Delta\mu_{Ca^{2+}/2H^+} = \mu^{in}_{Ca^{2+}} - 2\mu^{in}_{H^+} - \mu^{out}_{Ca^{2+}} + 2\mu^{out}_{H^+}. \quad (5)$$

We refer henceforth to the force associated with the exchange of ions as an osmotic force. The driving thermal force $(1/T^{in} - 1/T^{out})$ is given by the temperature difference over the membrane. The driving forces for the reaction and the exchange of ions are evaluated at the temperature of the lumen, T^{in} (22). The entropy production, σ, is (22)

$$\sigma = -r\frac{\Delta_r G}{T^{in}} - J_{Ca^{2+}}\frac{\Delta\mu_{Ca^{2+}/2H^+}}{T^{in}} + J'^{out}_q\left(\frac{1}{T^{in}} - \frac{1}{T^{out}}\right), \quad (6)$$

where, we note, the entropy production is still in a bilinear form even though the fluxes are nonlinear functions of the driving forces. This was also pointed out by Ross and Mazur in considering the entropy production of a chemical reaction (34).

The transport coefficients, D_{ij}, describe the coupling between the forces and fluxes. The efficiency of the pump in transferring calcium ions using the energy from the ATP hydrolysis is quantified through the coefficients D_{dr} and D_{rd}, which also describe the reverse situation, namely the synthesis of ATP using the energy stored in the chemical potential gradient of the ions. The coefficients D'_{qd} and D'_{qr} describe heat production due to the reaction or exchange of ions, whereas D'_{dq} and D'_{rq} describe how a temperature difference can drive the reaction and exchange of ions. These coefficients can be used to interpret nonshivering thermogenesis. The remaining coefficients, D_{dd}, D_{rr}, and D'_{qq}, describe the interdiffusion of the ions, the coupling of the reaction rate to the Gibbs energy of the reaction, and the thermal conductivity, respectively. Generally, the coefficients do not depend on the values of the forces or fluxes but may depend on state variables, e.g., temperature. Onsager reciprocal relations do not necessarily apply, but the coefficients are related. The origin of this is the coarse-graining on moving from the mesoscopic description to the macroscopic description: Onsager relations apply on the mesoscopic scale, but integration over the internal mesoscopic coordinates, yielding Eq. 3, leaves the transport coefficients asymmetric (22). Kjelstrup et al. (23) described both experiments to obtain the coefficients and estimated these coefficients for different isoforms of the Ca^{2+}-ATPase pump.

The equations we have given are valid for a nonisothermal case. However, most experiments of the pump are

performed without considering possible heat effects. This can be justified by estimating the contributions of the different terms of the entropy production. We do this in Table 1. We consider the data given for the reaction rate, flux of calcium ions, and heat flux in the supporting information of Kjelstrup et al. (23). During operation, the interior of the vesicle may cool, forming a temperature difference of 1 K over the vesicle (35). We see that in all cases, the contribution from the heat flux is small compared to the contribution from the reaction rate. In accordance with this, in the following, we neglect the contribution from the heat flux to entropy production, and we approximate $T = T^{\text{in}} \approx T^{\text{out}}$.

To quantify the thermodynamic efficiency of the system, we consider the lost work during the operation, W_{lost}, given by the Gouy-Stodola theorem (36),

$$W_{\text{lost}} = T_0\sigma, \tag{7}$$

where T_0 is the constant temperature of the system's surroundings. The expression above is general, meaning that it can be used for nonisothermal conditions and chemical reactions far from equilibrium (34). It is equal to the Clausius uncompensated heat for $T_0 = T$. If the system is not at the temperature of surroundings, the difference $T - T_0$ can be used to do work and/or dissipate energy. The entropy production of the system with $T = T^{\text{in}} \approx T^{\text{out}}$ is

$$\sigma = -r\frac{\Delta_r G}{T} - J_{Ca^{2+}}\frac{\Delta\mu_{Ca^{2+}/2H^+}}{T}. \tag{8}$$

The expression was derived using energy conservation along the transport path, an electroneutral exchange of ions (22), and a negligible thermal driving force. The last conditions are likely under the pump-operating conditions used (2,11,14–17,37,38). This expression was also used by Caplan and Essig (39), who considered the isothermal case and the linear regime of proper pathways. The maximum attainable work, W_{ideal}, is given by

$$W_{\text{ideal}} = -r\Delta_r G, \tag{9}$$

and the efficiency, η, of the pump can then be defined as

$$\eta = \frac{W_{\text{ideal}} - W_{\text{lost}}}{W_{\text{ideal}}} = \frac{-r\Delta_r G - T\sigma}{-r\Delta_r G} = \frac{J_{Ca^{2+}}\Delta\mu_{Ca^{2+}/2H^+}}{-r\Delta_r G}. \tag{10}$$

At reversible conditions, $(-r\Delta_r G = J_{Ca^{2+}}\Delta\mu_{Ca^{2+}/2H^+})$, $\eta = 1$ and the entropy production is zero. Equation 10 defines the thermodynamic efficiency in terms of measurable quantities. Caffrey and Feigenson (2) noted that the ratio $J_{Ca^{2+}}/r$ "is an index of the efficiency of the transport process". The calcium pump has two binding sites and can theoretically transport two calcium ions per ATP hydrolyzed. A pump where $J_{Ca^{2+}}/r = 2$ is referred to as a tight pump, whereas a pump where $J_{Ca^{2+}}/r<2$ is referred to as a slipping pump (40). The slippage depends on the driving forces; for larger forces (or rates), which correspond to larger entropy production, slippage becomes more likely (21). When $-\Delta_r G \approx 2\Delta\mu_{Ca^{2+}/2H^+}$, the ratio $(J_{Ca^{2+}}/r)/2$ can be used to estimate the efficiency, but this approximation is not accurate in general.

TABLE 1 Estimation of entropy production for experiments of Ca^{2+}-ATPases taken from various sources

Source of protein	Entropy production/μJ/mg protein × min × K			
	σ_r	$\sigma_{\Delta\mu}$	σ_q	η
WM	285 ± 20	−35 ± 4	1.82 ± 0.13	0.12 ± 0.02
BAT	60 ± 9	−4.0 ± 0.6	0.68 ± 0.14	0.067 ± 0.014
RM	52 ± 9	−6.0 ± 0.6	0.063 ± 0.011	0.12 ± 0.02
BP	10 ± 2	−1.0 ± 0.02	0.017 ± 0.002	0.13 ± 0.03
WM-HSR	540 ± 50	−14 ± 2	0.07 ± 0.05	0.026 ± 0.004

Protein sources are white muscle (WM) (11,15,16), brown adipose tissue (BAT) (14,16), red muscle (RM) (15), blood platelets (BP) (37,38), and white muscle heavy fraction (WM-HSR) (17). In the experiments, the initial rates for ATP hydrolysis, Ca^{2+}-transport, and heat were measured. We used the calculated fluxes and forces given in the supporting information of Kjelstrup et al. (23). The assay medium consists of (23) 50 mM Mops/Tris buffer (pH 7.0), 100 mM KCl, 1 mM ATP, 10 mM Pi, 2 mM $MgCl_2$, 10 μM $CaCl_2$, and 5 mM NaN_3. The free-Ca^{2+} concentration was 5 μM and the temperature was 35°C. We refer readers to the supporting information of Kjelstrup et al. (23) and references therein for further details regarding the experiments. The driving forces for the experimental conditions are $\Delta_r G = -46$ kJ/mol (23). Note that the change in Gibbs free energy of the ATP hydrolysis does not correspond to physiological conditions in these experiments. The concentration on the inside of the vesicles reaches the mM range a few seconds after transport is initiated (15), and this corresponds to a concentration ratio of the order 10^4. We use this value to estimate the change in chemical potential on moving the ions, $\Delta\mu_{Ca^{2+}/2H^+} = 24$ kJ/mol. We estimate the thermal driving force as a temperature difference of 1 K at 35°C: $(1/T^{\text{in}} - 1/T^{\text{out}}) \approx (1/307 - 1/308)\text{K}^{-1}$. For brevity, we define $\sigma_r \equiv -r\Delta_r G/T^{\text{in}}$, $\sigma_{\Delta\mu} \equiv -J_{Ca^{2+}}\Delta\mu_{Ca^{2+}/2H^+}/T^{\text{in}}$, and $\sigma_q \equiv J_q'^{\text{out}}(1/T^{\text{in}} - 1/T^{\text{out}})$ for the different contributions in the table headings. The uncertainties were calculated from the reported uncertainties in the experiments, as shown in Appendix A for the efficiency.

Evaluation of the driving forces

To evaluate the efficiency, we need to calculate the fluxes and the corresponding driving forces. We assume that the fluxes measured in the experiments (e.g., in Caffrey and Feigenson (2)) represent the average net fluxes for the duration of the experiment. During most experiments, calcium is transported from the outside to the inside of the vesicles as ATP is hydrolyzed. Since the concentration of the different species changes over time, we chose to calculate the driving forces as time averages over the duration of the experiments, Δt (0.5 min in the experiments reported in Caffrey and Feigenson (2)).

The osmotic driving force

Initially, the amount of calcium on the inside of the vesicles, n^{in} is zero and the amount of calcium on the outside is n_0^{out}.

We assume that the amount of calcium on the inside at any given time, t, is given by the flux of calcium ions:

$$n^{\text{in}}(t) = J_{Ca^{2+}} \times m_P \times t, \tag{11}$$

where m_P is the mass of protein in the solution, given by the volume of the solution, 0.25 mL, and the density of reconstituted protein in the solution, 19.2 μg protein/mL (2). We note that a deviation from the initial linear behavior of the Ca^{2+} uptake is expected for longer times of 10–20 min (see, for instance, Arruda et al. (15)). The amount of calcium on the outside is $n^{\text{out}}(t) = n_0^{\text{out}} - n^{\text{in}}(t)$. The osmotic driving force is calculated using Eq. 5, where we assume that the pH is identical on both sides, ($\mu^{\text{in}}_{H^+} \approx \mu^{\text{out}}_{H^+}$). Approximating the activities with concentrations we get

$$\begin{aligned}\Delta\mu_{Ca^{2+}/2H^+}(t) &= \mu^{\text{in}}_{Ca^{2+}} - \mu^{\text{out}}_{Ca^{2+}} = RT \ln \frac{[Ca^{2+}]^{\text{in}}}{[Ca^{2+}]^{\text{out}}} \\ &= RT \ln \frac{n^{\text{in}}(t)/V_{\text{in}}}{(n_0^{\text{out}} - n^{\text{in}}(t))/V_{\text{out}}},\end{aligned} \tag{12}$$

where V_{in} is the volume of the vesicle and V_{out} the volume of the solution. The volume of the vesicles depends on the experimental conditions and also on the uptake of Ca^{2+}. Beeler reported values of the order 1.1–7.4 μL/mg protein (41) for loaded vesicles. We choose to estimate the volume of the vesicles as $V_{\text{in}} = V_v \times m_P$, where $V_v = 5$ μL/mg protein (23). This value agrees with the one that can be inferred from the vesicle diameters reported by Caffrey and Feigenson (2) and with estimates of the surface concentration of proteins in cardiac SR vesicles, 10^4 proteins/μm^2 (42).

Averaging over the duration of the experiment, Δt (0.5 min (2)), we get

$$\begin{aligned}\frac{\langle \Delta\mu_{Ca^{2+}/2H^+} \rangle}{RT} &= \ln \frac{V_{\text{out}}}{V_{\text{in}}} + \frac{1}{\Delta t} \int_0^{\Delta t} \ln \frac{n^{\text{in}}(t)}{n_0^{\text{out}} - n^{\text{in}}(t)} \mathrm{d}t \\ &= \ln \frac{V_{\text{out}}}{V_{\text{in}}} + \frac{1}{f} \ln(1-f) - \ln(1/f - 1),\end{aligned} \tag{13}$$

where $0 < f = n^{\text{in}}(\Delta t)/n_0^{\text{out}} < 1$.

Evaluation of driving force for the reaction

The driving force for the reaction is calculated using

$$\begin{aligned}\Delta_r G &= \mu_{ADP} + \mu_{Pi} - \mu_{ATP} - \mu_{H_2O} = \Delta_r G^{\ominus} + RT \ln \frac{a_{ADP} a_{Pi}}{a_{ATP}} \\ &= \Delta_r G^{\ominus} + RT \ln \frac{[ADP][Pi]}{[ATP]},\end{aligned} \tag{14}$$

where the activity coefficients have been included in the definition of $\Delta_r G^{\ominus}$. At the experimental conditions (see Caffrey and Feigenson (2)), $T = 298.15$ K, pH 7.5, pMg 2.3, and ionic strength 66.3 mM, we find $\Delta_r G^{\ominus} = -32.61$ kJ/mol, according to the approach of Alberty (25), which gives the Gibbs energy of the ATP hydrolysis as a function of temperature, pH, pMg, and ionic strength.

We evaluate the average driving force, using the averaged rate of hydrolysis, r, in a way similar to the approach used for the exchange of ions. In this case,

$$[ADP] = [Pi] = \frac{n(t)}{V_{\text{out}}}, [ATP] = \frac{n_{ATP,0} - n(t)}{V_{\text{out}}}, \tag{15}$$

where

$$n(t) = r \times m_p \times t \tag{16}$$

and $n_{ATP,0}$ is the initial amount of ATP in the solution.

Averaging over the duration of the experiment, Δt (0.5 min (2)),

$$\begin{aligned}\frac{\langle \Delta_r G \rangle}{RT} &= \frac{\Delta_r G^{\ominus}}{RT} + \frac{1}{\Delta t} \int_0^{\Delta t} \ln \frac{n(t)^2}{V_{\text{out}}(n_{ATP,0} - n(t))} \mathrm{d}t \\ &= \frac{\Delta_r G^{\ominus}}{RT} + \ln \frac{n(\Delta t)}{V_{\text{out}}} - 1 + \frac{1}{f'} \ln(1-f') - \ln(1/f' - 1),\end{aligned} \tag{17}$$

where $0 < f' = n(\Delta t)/n_{ATP,0} < 1$.

THERMODYNAMIC EFFICIENCY

We have calculated the entropy production and the thermodynamic efficiency (see Table 2) of the calcium pump reconstituted in membranes of different composition and thickness, as investigated in the experiments of Caffrey and Feigenson (2). Figs. 2 and 3 give the entropy production and the thermodynamic efficiency of the pump, respectively, for the different experiments. We find that the driving force for the reaction is large, ~ 80 kJ/mol (Eq. 17), whereas the osmotic driving force is smaller (~ -10 kJ/mol) (Eq. 13). We also find that $-\Delta_r G > \Delta\mu_{Ca^{2+}/2H^+}$ in all cases, giving a negative net change in Gibbs energy for the whole process. In all cases (see Table 2), $J_{Ca^{2+}}/r < 1$, which means that, on average, more than one ATP molecule is needed to transport one calcium ion. This might be connected to the futile operation of the pump (ATP hydrolysis without transporting calcium ions) or to leakage of calcium ions from the vesicle in such a way that ATP is not regenerated. The leakage might proceed through pathways that do not involve Ca^{2+}-ATPase (40). Ratios of $J_{Ca^{2+}}/r$ close to 2 are, according to Berman (40), only observed when the concentration on the inside of the vesicles is relatively small, <50 μM (21). For comparison, all the averaged concentrations we calculate are of the order 3–35 mM,

TABLE 2 Calculated entropy production and efficiency for the calcium pump embedded in vesicles of different phosphatidylcholine type

Phosphatidylcholine type	Acyl chain length	$J_{Ca^{2+}}/r$	Entropy production (Eq. 8)/(μJ/mg protein × min × K)	Efficiency (Eq. 10)
Myristelaidic	14	0.75	11.9 ± 1.3	0.048 ± 0.012
Myristoleic	14	0.50	40 ± 4	0.046 ± 0.011
Palmitelaidic	16	0.20	220 ± 20	0.026 ± 0.006
Palmitoleic	16	0.43	180 ± 20	0.064 ± 0.016
Elaidic	18	0.36	270 ± 30	0.057 ± 0.014
Linoleic	18	0.39	320 ± 30	0.067 ± 0.016
Oleic	18	0.38	290 ± 30	0.063 ± 0.015
Petroselaidic	18	0.37	180 ± 20	0.052 ± 0.013
Vaccenic	18	0.33	320 ± 30	0.055 ± 0.013
Eicosenoic	20	0.66	200 ± 20	0.11 ± 0.03
Erucic	22	0.52	300 ± 30	0.09 ± 0.02
Nervonic	24	0.30	156 ± 17	0.040 ± 0.009

Calculations are based on the experimental data of Caffrey and Feigenson (2), and the ratios of the flux of calcium ions to the rate of the hydrolysis reaction ($J_{Ca^{2+}}/r$) given in this table are reproduced from the same source (2). The maximum value for this ratio is 2, since the calcium pump has two binding sites. The uncertainties were estimated as described in Appendix A.

which is much higher, pointing toward a possible inhibitory effect of Ca^{2+}.

The entropy production quantifies the amount of heat released during the pump operation. Fig. 2 shows that the entropy production rises quickly from short (~14) to long (~18) acyl chain lengths and remains more or less constant for even longer acyl chains. We have compared the heat production from reconstituted ATPases, estimated from NET and the experimental data, with different calorimetric experiments, which provide estimates of the heat released during the pump operation when the ATPase is embedded in vesicles from the SR (10–16). Our estimate for the entropy production should be compared in the first instance with the calorimetric experiments of ATPase extracted from white muscle, as these are the proteins used in the studies of Caffrey and Feigenson (2). As shown in Fig. 2, our predictions using NET theory are in good agreement with the direct measurements of heat dissipation. This is surprising given the different conditions for the ATPase in the two cases, e.g., that the ATPase derived from the SR may benefit from proton leaks through the membrane, whereas this may not be the case for the reconstituted pump (2).

We have also applied our analysis to other ATPases extracted from different tissues (see Table 1 and Fig. 2). We find that the entropy production, or heat dissipation, features a strong dependence on the ATPase source, being very small for red muscle and blood platelet ATPases.

The low values of $J_{Ca^{2+}}/r$ are reflected in the low efficiency calculated for the pump. As noted previously, slippage is expected to be bigger for larger forces, and our

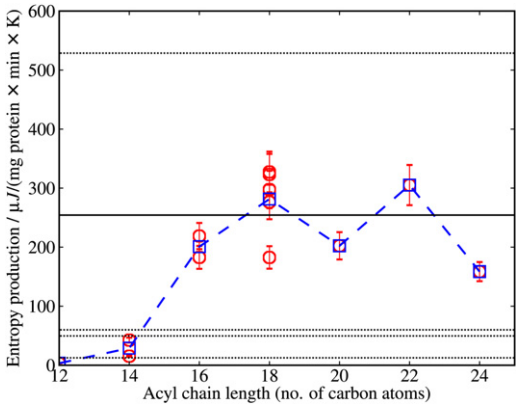

FIGURE 2 Entropy production (*circles*) of the system as a function of acyl chain length, calculated using Eq. 8 and the experimental data of Caffrey and Feigenson (2), as listed in Table 2. The uncertainties have been estimated as explained in Appendix A. The average values (*squares*) are calculated for each chain length and are connected with a dashed line. Horizontal lines represent estimates of the entropy production for the ATPases listed in Table 1, from top to bottom: white muscle heavy fraction, white muscle, brown adipose tissue, red muscle, and blood platelets. We note that the experiments by Caffrey and Feigenson (2) were carried out at 25°C, whereas the experiments listed in Table 1 were carried out at 35°C.

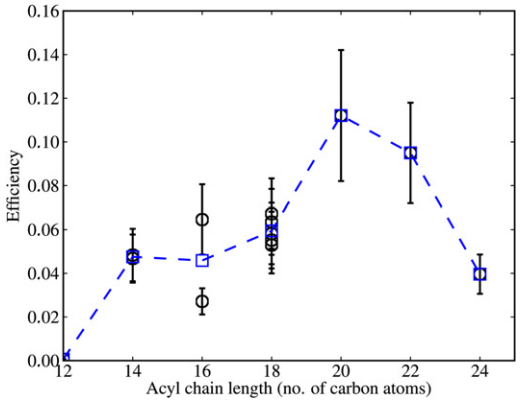

FIGURE 3 Efficiency (*circles*) of the system as a function of acyl chain length. The efficiencies are calculated using Eq. 10 and the experimental data of Caffrey and Feigenson (2) and are listed in Table 2. The uncertainties have been estimated as explained in Appendix A. The average values (*squares*) are calculated for each chain length and are connected with a dashed line.

results for the efficiency are consistent with the relatively large driving force for the reaction. Hence, larger slippage reduces the efficiency. The efficiency is larger for acyl chain lengths in the range 18–22 carbon atoms, which coincides with the maximum in the protein activity, measured in terms of Ca^{2+} transport and ATP hydrolysis (2). The efficiency estimated from these experimental data is surprisingly low, only ~12%. It may be hampered by a reduced possibility for proton transport, although this is not evident from the SR data. The efficiency is still low for proteins extracted from different sources (see Table 1 and Fig. 2), and can even be lower than the one estimated above for the white muscle case. It varies significantly with the tissue.

CONCLUSIONS AND FINAL REMARKS

Nonequilibrium thermodynamics theory provides a route to estimate the thermodynamic efficiency of the Ca^{2+} pump by analyzing experimental data. The approach presented in this article requires information on Ca^{2+} flux and the ATP hydrolysis rate. Both quantities are experimentally accessible. Using the experimental data in combination with NET equations, it is possible to estimate the pump efficiency and also the entropy production. The entropy production estimated from our NET theoretical approach shows good agreement with the available calorimetric experiments for Ca^{2+}-ATPase in SR vesicles. This gives us confidence as to the approximations used in the derivation.

One objective of this work was to estimate the thermodynamic efficiency of the Ca^{2+}-ATPase as a function of the structure of the supporting membrane. Previous experimental studies using phospholipid vesicles of different compositions have indicated that the pump activity strongly depends on the bilayer thickness (2). This activity reaches a maximum for phospholipid acyl chain lengths of between 18 and 20 carbon atoms. We find that the thermodynamic efficiency also reaches a maximum for this interval of acyl chain lengths, with a concomitant increase in heat dissipation (entropy production). We find that ATPases extracted from white muscle lead to higher entropy production and heat dissipation, but also to higher thermodynamic efficiency.

Interestingly, we have found that the thermodynamic efficiency is very low for all the cases we analyzed. The efficiency for ATPases extracted from different sources, white and red muscle or blood platelets, never reaches values >13%. This is a remarkably small value for the efficiency of a pump, or a nanopump in our case. The low efficiency we have estimated here might be affected by the experimental conditions and the ATPase preparation procedure. The preparation procedure likely has a negative impact on the state of the pump, as it is obtained through disruption and self-assembly of the vesicle material. For this reason alone, one may expect a higher efficiency in vivo.

Also, in a biological environment, the ATPase might operate under stationary conditions and with large Ca^{2+} concentration gradients. In the experiments analyzed in this article, the concentration inside the vesicles might reach large values, >1 mM, large enough to inhibit the functioning of the pump. Concentration gradients under optimal biological conditions are estimated to be very high, 40,000:1 (see Møller et al. (43)). Considering this concentration gradient and ratios of $J_{Ca^{2+}}/r \sim 2$, it is easy to see that the thermodynamic efficiency of the pump might increase significantly (44). We point out, however, that the efficiency will depend strongly on variations in the Ca^{2+} gradient magnitude, as can be inferred from the strong dependence of the ATPase turnover activity with Ca^{2+} uptake (see Møller et al. (43)).

The efficiencies obtained here for Ca^{2+}-ATPase are far from those reported recently for ATP-fueled rotary nanomotors, where values near 100% have been suggested (45). Our work implies that the efficiency of ATPase nanomachines can be very sensitive to experimental conditions, and that significant dissipation may occur during the nanomachine operation. Hence, we expect that very high efficiencies would be unlikely. Indeed, from the analysis of experimental data for kinesin, a motor protein powered by the hydrolysis of ATP, one can infer much lower efficiencies, ~50% (46,47). Other studies have reported even lower efficiencies for Brownian motors (48).

Finally, we note that the approach presented here is general and might be used to estimate thermodynamic efficiencies and heat dissipation of other nanomachines that use ATP as fuel to drive ion transport.

APPENDIX A: UNCERTAINTIES

We calculated the entropy production and efficiency as a function of the bilayer length using Eqs. 8, 10, 13, and 17 and the experimental data of Caffrey and Feigenson (2). By considering propagation of errors (49), we estimate the uncertainties in the entropy production, ε_σ, and efficiency, ε_η, by

$$\varepsilon_\sigma^2 = \left(\frac{r\varepsilon_{\Delta_r G}}{T}\right)^2 + \left(\frac{\Delta_r G \varepsilon_r}{T}\right)^2 + \left(\frac{\Delta\mu_{Ca^{2+}/2H^+}\varepsilon_{J_{Ca^{2+}}}}{T}\right)^2 + \left(\frac{J_{Ca^{2+}}\varepsilon_{\Delta\mu_{Ca^{2+}/2H^+}}}{T}\right)^2,$$

$$\left(\frac{\varepsilon_\eta}{\eta}\right)^2 = \left(\frac{\varepsilon_{J_{Ca^{2+}}}}{J_{Ca^{2+}}}\right)^2 + \left(\frac{\varepsilon_r}{r}\right)^2 + \left(\frac{\varepsilon_{\Delta_r G}}{\Delta_r G}\right)^2 + \left(\frac{\varepsilon_{\Delta\mu_{Ca^{2+}/2H^+}}}{\Delta\mu_{Ca^{2+}/2H^+}}\right)^2, \quad \text{(A1)}$$

where $\varepsilon_{J_{Ca^{2+}}}$, ε_r, $\varepsilon_{\Delta_r G}$, and $\varepsilon_{\Delta\mu_{Ca^{2+}/2H^+}}$ are the uncertainties in $J_{Ca^{2+}}$, r, $\Delta_r G$, and $\Delta\mu_{Ca^{2+}/2H^+}$, respectively. Unfortunately, the reported $J_{Ca^{2+}}/r$ values (2) are given without uncertainties. To comment on the uncertainties in our calculated values, we assume the uncertainties in these fluxes to be of the order of 10%. Further, we assume that the uncertainties in the concentrations in the assay medium are negligible. Based on this, we then neglect the contribution to the uncertainties from the estimation of the driving force of the reaction. We estimate the uncertainty in the driving force for the exchange of ions as arising from the uncertainty in the vesicle volume.

By considering different vesicle volumes as reported by Beeler (41), we estimate this uncertainty to be of the order of 20% of the calculated driving force in all cases. On calculating the uncertainties in the efficiency and entropy production, we obtain uncertainties of $\approx 30\%$ for the efficiency and $\approx 10\%$ for the entropy production.

We note that the assumption of ideal solutions in connection with the exchange of ions (see Eq. 13) corresponds to neglecting a contribution to the driving force of size $RT \ln \gamma^{out}_{Ca^{2+}}/\gamma^{in}_{Ca^{2+}}$, where $\gamma^{l}_{Ca^{2+}}$ denotes the activity coefficient for Ca^{2+} in phase 1. Considering the Debye-Hückel law, we estimate this contribution to the driving force to be of the order $\left|RT \ln \gamma^{out}_{Ca^{2+}}/\gamma^{in}_{Ca^{2+}}\right| < 1$ kJ/mol. This is $<10\%$ of the calculated driving force in all cases. This is a systematic error and will not alter the calculated values significantly, i.e., the error associated with the vesicle volume is larger.

A.L. thanks The Faculty of Natural Sciences and Technology, Norwegian University of Science and Technology, for a Ph.D. scholarship. F.B. thanks the Engineering and Physical Sciences Research Council of the UK for the award of a Leadership Fellowship. J.M.R acknowledges support from the Institució Catalana de Recerca i Estudis Avançats Academia Program.

REFERENCES

1. Berg, J. M., J. L. Tymoczko, and L. Stryer. 2002. Biochemistry, 5th ed. W. H. Freeman, New York.
2. Caffrey, M., and G. W. Feigenson. 1981. Fluorescence quenching in model membranes. 3. Relationship between calcium adenosinetriphosphatase enzyme activity and the affinity of the protein for phosphatidylcholines with different acyl chain characteristics. *Biochemistry.* 20:1949–1961.
3. Lee, A. G. 1998. How lipids interact with an intrinsic membrane protein: the case of the calcium pump. *Biochim. Biophys. Acta.* 1376:381–390.
4. Andersen, O. S., and R. E. Koeppe, 2nd. 2007. Bilayer thickness and membrane protein function: an energetic perspective. *Annu. Rev. Biophys. Biomol. Struct.* 36:107–130.
5. Jensen, M. O., and O. G. Mouritsen. 2004. Lipids do influence protein function—the hydrophobic matching hypothesis revisited. *Biochim. Biophys. Acta.* 1666:205–226.
6. Lervik, A., F. Bresme, and S. Kjelstrup. 2012. Molecular dynamics simulations of the Ca^{2+}-pump: a structural analysis. *Phys. Chem. Chem. Phys.* 14:3543–3553.
7. Sonntag, Y., M. Musgaard, …, L. Thøgersen. 2012. Mutual adaptation of a membrane protein and its lipid bilayer during conformational changes. *Nat. Commun.* 2:304.
8. MacLennan, D. H. 1970. Purification and properties of an adenosine triphosphatase from sarcoplasmic reticulum. *J. Biol. Chem.* 245:4508–4518.
9. Sugita, Y., N. Miyashita, …, C. Toyoshima. 2005. Protonation of the acidic residues in the transmembrane cation-binding sites of the Ca^{2+} pump. *J. Am. Chem. Soc.* 127:6150–6151.
10. de Meis, L., M. L. Bianconi, and V. A. Suzano. 1997. Control of energy fluxes by the sarcoplasmic reticulum Ca^{2+}-ATPase: ATP hydrolysis, ATP synthesis and heat production. *FEBS Lett.* 406:201–204.
11. de Meis, L. 2001. Uncoupled ATPase activity and heat production by the sarcoplasmic reticulum Ca^{2+}-ATPase. Regulation by ADP. *J. Biol. Chem.* 276:25078–25087.
12. de Meis, L. 2002. Ca^{2+}-ATPases (SERCA): energy transduction and heat production in transport ATPases. *J. Membr. Biol.* 188:1–9.
13. Barata, H., and L. de Meis. 2002. Uncoupled ATP hydrolysis and thermogenic activity of the sarcoplasmic reticulum Ca^{2+}-ATPase: coupling effects of dimethyl sulfoxide and low temperature. *J. Biol. Chem.* 277:16868–16872.
14. de Meis, L. 2003. Brown adipose tissue Ca^{2+}-ATPase: uncoupled ATP hydrolysis and thermogenic activity. *J. Biol. Chem.* 278:41856–41861.
15. Arruda, A. P., W. S. Da-Silva, …, L. De Meis. 2003. Hyperthyroidism increases the uncoupled ATPase activity and heat production by the sarcoplasmic reticulum Ca^{2+}-ATPase. *Biochem. J.* 375:753–760.
16. de Meis, L., G. M. Oliveira, …, M. Benchimol. 2005. The thermogenic activity of rat brown adipose tissue and rabbit white muscle Ca^{2+}-ATPase. *IUBMB Life.* 57:337–345.
17. Arruda, A. P., M. Nigro, …, L. de Meis. 2007. Thermogenic activity of Ca^{2+}-ATPase from skeletal muscle heavy sarcoplasmic reticulum: The role of ryanodine Ca^{2+} channel. *Biochim. Biophys. Acta.* 1768:1498–1505.
18. Suzuki, M., V. Tseeb, …, S. Ishiwata. 2007. Microscopic detection of thermogenesis in a single HeLa cell. *Biophys. J.* 92:L46–L48.
19. Bresme, F., A. Lervik, …, S. Kjelstrup. 2008. Water polarization under thermal gradients. *Phys. Rev. Lett.* 101:020602.
20. Römer, F., F. Bresme, …, J. M. Rubí. 2012. Thermomolecular orientation of nonpolar fluids. *Phys. Rev. Lett.* 108:105901.
21. Kjelstrup, S., J. M. Rubi, and D. Bedeaux. 2005. Energy dissipation in slipping biological pumps. *Phys. Chem. Chem. Phys.* 7:4009–4018.
22. Bedeaux, D., and S. Kjelstrup. 2008. The measurable heat flux that accompanies active transport by Ca^{2+}-ATPase. *Phys. Chem. Chem. Phys.* 10:7304–7317.
23. Kjelstrup, S., D. Barragán, and D. Bedeaux. 2009. Coefficients for active transport and thermogenesis of Ca^{2+}-ATPase isoforms. *Biophys. J.* 96:4376–4386.
24. Alberty, R. A., and R. N. Goldberg. 1992. Standard thermodynamic formation properties for the adenosine 5′-triphosphate series. *Biochemistry.* 31:10610–10615.
25. Alberty, R. A. 2003. Thermodynamics of the hydrolysis of adenosine triphosphate as a function of temperature, pH, pMg, and ionic strength. *J. Phys. Chem. B.* 107:12324–12330.
26. Niggli, V., and E. Sigel. 2008. Anticipating antiport in P-type ATPases. *Trends Biochem. Sci.* 33:156–160.
27. Palmgren, M. G., and P. Nissen. 2011. P-type ATPases. *Annu. Rev. Biophys.* 40:243–266.
28. Garcia, A. M., and C. Miller. 1984. Channel-mediated monovalent cation fluxes in isolated sarcoplasmic reticulum vesicles. *J. Gen. Physiol.* 83:819–839.
29. Kamp, F., P. Donoso, and C. Hidalgo. 1998. Changes in luminal pH caused by calcium release in sarcoplasmic reticulum vesicles. *Biophys. J.* 74:290–296.
30. Meissner, G. 1981. Calcium transport and monovalent cation and proton fluxes in sarcoplasmic reticulum vesicles. *J. Biol. Chem.* 256:636–643.
31. Tran, K., N. P. Smith, …, E. J. Crampin. 2009. A thermodynamic model of the cardiac sarcoplasmic/endoplasmic Ca^{2+} (SERCA) pump. *Biophys. J.* 96:2029–2042.
32. Yu, X., S. Carroll, …, G. Inesi. 1993. H^+ countertransport and electrogenicity of the sarcoplasmic reticulum Ca^{2+} pump in reconstituted proteoliposomes. *Biophys. J.* 64:1232–1242.
33. Reguera, D., J. M. Rubí, and J. M. G. Vilar. 2005. The mesoscopic dynamics of thermodynamic systems. *J. Phys. Chem. B.* 109:21502–21515.
34. Ross, J., and P. Mazur. 1961. Some deductions from a formal statistical mechanical theory of chemical kinetics. *J. Chem. Phys.* 35:19–28.
35. Kjelstrup, S., L. de Meis, …, J. M. Simon. 2008. Is the Ca^{2+}-ATPase from sarcoplasmic reticulum also a heat pump? *Eur. Biophys. J.* 38:59–67.
36. Kjelstrup, S., D. Bedeaux, …, J. Gross. 2010. Non-Equilibrium Thermodynamics for Engineers. World Scientific, Toh Tuck Link, Singapore.
37. Benech, J. C., H. Wolosker, and L. de Meis. 1995. Reversal of the Ca^{2+} pump of blood platelets. *Biochem. J.* 306:35–38.

38. Mitidieri, F., and L. de Meis. 1999. Ca^{2+} release and heat production by the endoplasmic reticulum Ca^{2+}-ATPase of blood platelets. Effect of the platelet activating factor. *J. Biol. Chem.* 274:28344–28350.

39. Caplan, S. R., and A. Essig. 1999. Bioenergetics and Linear Nonequilibrium Thermodynamics: The Steady State. Harvard University Press, Cambridge, MA.

40. Berman, M. C. 2001. Slippage and uncoupling in P-type cation pumps; implications for energy transduction mechanisms and regulation of metabolism. *Biochim. Biophys. Acta.* 1513:95–121.

41. Beeler, T. 1983. Osmotic changes of sarcoplasmic reticulum vesicles during Ca^{2+} uptake. *J. Membr. Biol.* 76:165–171.

42. Beca, S., E. Pavlov, …, G. J. Kargacin. 2008. Inhibition of a cardiac sarcoplasmic reticulum chloride channel by tamoxifen. *Pflugers Arch.* 457:121–135.

43. Møller, J. V., C. Olesen, …, P. Nissen. 2010. The sarcoplasmic Ca^{2+}-ATPase: design of a perfect chemi-osmotic pump. *Q. Rev. Biophys.* 43:501–566.

44. Läuger, P. 1991. Electrogenic Ion Pumps. Sinauer, Sunderland, MA.

45. Kinosita, Jr., K., R. Yasuda, …, K. Adachi. 2000. A rotary molecular motor that can work at near 100% efficiency. *Philos. Trans. R. Soc. Lond. B Biol. Sci.* 355:473–489.

46. Bustamante, C., J. Liphardt, and F. Ritort. 2005. The nonequilibrium thermodynamics of small systems. *Phys. Today.* 58:43–48.

47. Kawaguchi, K. 2008. Energetics of kinesin-1 stepping mechanism. *FEBS Lett.* 582:3719–3722.

48. Astumian, R. D. 1997. Thermodynamics and kinetics of a Brownian motor. *Science.* 276:917–922.

49. Bevington, P. R., and D. K. Robinson. 2003. Data Reduction and Error Analysis for the Physical Sciences, 3rd ed. McGraw-Hill, New York.